Dynamical lattice-model simulation

John R. Gunn,* C. Michael McCallum, and K. A. Dawson†
Department of Chemistry, University of California, Berkeley, Berkeley, California 94720
(Received 16 August 1991; revised manuscript received 8 September 1992)

We present an algorithm for carrying out time-dependent canonical Monte Carlo simulations on a lattice with single occupancy of each site and arbitrary site-site interactions. The method incorporates velocities at each site whose components are proportional to the probability of exchange with each of the neighboring sites. Kinetic and potential energy are exchanged through the choice of trial final velocities for attempted exchanges which are accepted or rejected using the Metropolis algorithm. Caculations are carried out for the two-dimensional Ising model for which the exact partition function is known. Our method reproduces the results of standard Monte Carlo simulations with comparable accuracy, and in addition allows the calculation of dynamical properties previously inaccessible with traditional methods. Results are presented for self-diffusion, interfacial tension, and shear viscosity.

PACS number(s): 05.50.+q, 66.10.Cb, 68.10.Cr

I. INTRODUCTION

In the modeling and computer simulation of complex classical fluids, it is often necessary to compromise between the detail required to describe interesting physical phenomena and the simplicity required for computational efficiency. There are two principal methods currently in use, molecular dynamics and Monte Carlo, each of which has advantages and disadvantages [1].

Molecular-dynamics (MD) calculations provide the most complete information on the system, and have the advantage of being an essentially exact solution of the classical equations of motion with constant energy and volume. MD simulations thus have an explicit time dependence and can be used to calculate both static and dynamic properties of a system. This method can also be modified to simulate constant temperature and pressure ensembles and to simulate nonequilibrium conditions such as shear flow. The practical limitations of MD arise from the need to calculate continuous forces and torques and to integrate the equations of motion using a very short (typically $\sim 10^{-15}$ s) time step. For a system containing multiple components of different sizes and rapidly varying forces on a number of length scales, the simulation may be very slow relative to motion of interest and it may be difficult to obtain accurate ensemble averages. Methods such as the use of multiple time steps and coordination shells can reduce these problems, but they remain a significant limitation. Furthermore, in systems with longer-ranged forces it may require a very large number of particles to simulate a system larger than all potential cutoff distances and relevant correlation lengths.

These difficulties can be partially overcome in Monte Carlo (MC) simulations. In this case there is no meaningful time and it is not necessary to calculate forces. The configuration is updated according to the potential energy alone, and in principle there is no limitation on the types of moves that may be attempted. This method has the advantage of being computationally simpler, and being able to sample configuration space much more efficiently. It also allows moves which are "unphysical" such as particle insertion in a grand-canonical simulation. It has the major drawback of not being able to calculate any time-dependent quantities such as velocity and pressure autocorrelation functions. Methods exist such as force-bias Monte Carlo and Langevin dynamics which combine elements of MC and MD for continuum systems; however, one major application of the MC method is for discrete lattice models for which there is no analog of MD in the sense that there are no continuous equations of motion that can be integrated. Lattice models lack the detailed interaction of continuum models, but their simplicity makes them very well suited for computer simulation where the calculation of the potential energy can be made highly efficient. Since the range of interactions is typically only one or two lattice spacings, it is easy to carry out simulations which are large relative to the important correlation lengths, even for highly complex or near-critical systems. Furthermore, the discrete motions of the particles are in steps on the order of the molecular diameter, which would take a large number of iterations to achieve in a continuous system. Although such a coarse-grained model sacrifices much of the microscopic detail of real molecules, there are many systems where the interesting behavior occurs on time scales and length scales for which this is the only tractable approach.

In particular, the present work was inspired by a lattice model of microemulsion recently developed by the present authors [2]. Despite greatly simplified interactions, the model reproduces a large number of complex phases and microstructures found experimentally. It is of considerable interest to calculate dynamical and nonequilibrium properties of such a system, but continuum MD calculations even with very crude potential functions have proven to be very difficult and time consuming [3], and with more detailed models it is almost impossible to simulate a system large enough and over long enough times to study equilibrium phase behavior [4]. Our goal

is to incorporate into the existing lattice model realistic motions and time dependence to allow calculation of dynamical properties of the system which are not currently accessible. We also require that the equilibrium state of the dynamical model should coincide with that of the original lattice model.

Recently, much work has been done in developing lattice-gas cellular-automaton (LGCA) models [5] based on the pioneering work of Frisch, Hasslacher, and Pomeau [6] (FHP) in which the sites on a lattice possess discretized velocities which specify the neighboring site to which each particle will move during the following time step. In models of this type, there is a small density of occupied sites which propagate into neighboring vacant sites. If two or more particles move to the same vacant site, they collide, and simple collision rules are used to specify the directions in which they leave the site in the next step, thus including elastic scattering in the model. Multiply occupied sites are allowed subject to the condition that each particle on a site have a unique velocity. Variations also exist in which there are rest particles, higher mass particles, and diagonal (higher speed) moves. The power of this method lies in its computational simplicity. It is a true cellular automaton, since the state (occupation and velocities) of a site is uniquely determined by the states of its neighbors in the previous step, and can thus be programmed using very efficient parallel and vector algorithms based on integer arithmetic. As a result, very large systems can be simulated, and it has been shown that upon coarse graining the model reproduces hydrodynamic behavior described by the Navier-Stokes equation.

Another method has been developed, maximally discretized molecular dynamics (MDMD) [7], in which the particles behave as hard hexagons and are constrained to single occupancy on a triangular lattice. If a particle attempts to move to an occupied site, it remains at its original site and the velocities of the two colliding particles are scattered prior to the next move. The moves are attempted sequentially, and clusters of three or more particles are dealt with in random order as a series of pairwise collisions. The model is thus a crude description of a dense fluid, but at low densities of occupied sites it reproduces the behavior of hard disks with orders of magnitude less computing time than standard MD simulations.

These models are limited, however, by the fact that they describe explicitly "hard" particles, and possess no potential energy. Realistic fluid behavior is thus obtained solely from the simple collision rules that specify the model. Our aim then is to extend the idea of site velocities on a lattice to the case where the particles interact via an Ising-type lattice Hamiltonian, and thus bridge the gap between MC and MD simulations for models described on a lattice.

II. DEVELOPMENT OF THE DYNAMICAL MC ALGORITHM

The fundamental difference between our approach and that of previous LCGA models is thus the inclusion of nontrivial interparticle interactions. Some researchers have developed models with primitive interactions that possess phase transitions and phase boundaries [8], however, by introducing a meaningful temperature (or energy scale) they are necessarily no longer purely deterministic, but possess collisions with temperature-dependent random outcomes. Furthermore, in order for the potential energy to be defined by an Ising-type Hamiltonian it is necessary that each site be occupied by exactly one particle or state. The condition that there be no vacant or multiply occupied sites immediately implies that the motions of the particles cannot be independent. That is, any movement must be in a closed loop of two or more sites such that the occupation of each site is conserved. This introduces to the system a frustration in the sense that the deterministic motions of the particles cannot be simultaneously satisfied within this constraint. This is a significant distinction between the present problem and LGCA or MD algorithms. It means that any velocities attributed to the lattice sites cannot uniquely determine the motions of the particles independently of the other site velocities. Methods have been proposed to address this issue in which the selected exchange of particles is optimized in some sense [9], however, in the present model we wish to have not the optimal outcome of collisions, but rather a Boltzmann distribution of all possible outcomes. Again, this requires collision rules that are probabilistic in nature. A method has been proposed [10] in which the random outcomes are "frozen" in advance resulting in a deterministic simulation; however, this creates a frustrated system which fails to reproduce equilibrium structure.

For simplicity, we consider only the exchange of nearest-neighbor sites as the basic update of the lattice. Each time step thus consists of a trial exchange of each pair of nearest neighbors in the lattice. These are considered to be independent and are updated in a pseudorandom sequence. Since the neighbors of each pair are required in the evaluation of the potential energy, nearby pairs are not actually independent. The update sequence must ensure that dependent pairs are not updated simultaneously and this can be achieved by dividing the lattice into noninteracting sets of paired sites in a parallel computation [11]. The fact that each site has several neighbors with which it must be separately paired can be dealt with in a similar manner.

The necessary "collision" rules can thus be reduced to a decision of whether or not to exchange a specified pair of sites. A method has been introduced by Creutz [12], in which a kinetic energy is assigned to each site on a lattice and single spin flips are carried out if the kinetic energy is larger than the increase in potential energy for the spin flip. This model is completely deterministic, simply by specifying that the total energy is conserved in each spin flip and that all possible spin flips will be made. We propose to consider a pair of sites in a similar fashion, where the kinetic energy of the pair can be used to supply the potential energy required for an exchange. Accordingly, we define the site velocity v as an internal variable which possesses an energy, $\frac{1}{2}mv^2$, that is in equilibrium with the potential energy of the lattice at a specified temperature.

This is interpreted as a kinetic energy with $\langle \frac{1}{2}mv^2 \rangle = k_B T$. In this way, the velocities can be regarded as a heat bath or energy reservoir coupled to the lattice which leads to more realistic dissipation of the configurational energy.

The requirement that the dynamical model duplicate the equilibrium properties of the system as defined by the conventional Hamiltonian implies that the distribution of configurations must be according to the Boltzmann probability which is determined by the potential energy as in a standard MC simulation. Combined with the required Boltzmann distribution of total energies, this implies a Maxwell-Boltzmann distribution of velocities. The total energy distribution is thus factored into its kinetic and potential parts. This distribution is specified by using the Metropolis algorithm to accept or reject trial changes in the total energy. As a result, a choice of trial velocities which preserves the Maxwell-Boltzmann distribution will also imply the correct distribution of the potential energy.

The change in potential energy is determined by the configuration, so the selection of a trial change in total energy allows us the freedom to select the amount of energy that can be exchanged between the kinetic and potential components. This freedom can be used to enforce an additional condition on the choice of velocities. Since we are interested in the motions of the sites, we choose to specify that the probability of a site moving in a given direction be proportional to the component of its velocity in that direction. This condition, along with the definition of kinetic energy, identifies the velocities introduced in the model with the properties of real velocities to the extent permitted by the constraints outlined above. These velocities determine the number of time steps required, on average, for the particle (or particles) on a site to move (by whatever mechanism) to a specified neighboring site. Any connection between this velocity and the real particle velocities on a scale smaller than a lattice spacing is less clear and will not be addressed here.

For any trial exchange, we need only consider the component of the velocity in the direction of the proposed motion, namely, the lattice vector separating the sites. This is equivalent to the assumption that any forces between the sites act along this axis. In addition, since the probability of an exchange must take into account both of the individual probabilities for each site to move into the position of the other, we consider the relative velocity between the sites as the basis for determining the exchange probability. Leaving the center-of-mass velocity unchanged trivially enforces the required conservation of linear momentum for the exchange, which preserves the condition that $\langle v \rangle = 0$. The resulting trial velocities can thus be described by a single scalar quantity, the component of the relative velocity along the axis of the pair, with all other components of the velocities conserved.

The master equation for the relative velocity in equilibrium can be written

$$\frac{dP(v)}{dt} = \int_0^\infty dv'[P(v')W(v' \to v) - P(v)W(v \to v')] = 0 , \tag{1}$$

where $P(v)$ is the probability of a pair having relative velocity v and $W(v \to v')$ is the transition probability for the velocity to change from v to v'. Since we wish to have the trial final velocity uniquely determined by the initial velocity we can write it as some, as yet unknown, $f(v)$, and thus

$$W(v \to v') \propto v\delta(v' - f(v)) , \tag{2}$$

which states that the probability of exchange is proportional to v, subject to the constraint that $v' = f(v)$.

In addition, we wish to introduce a condition of microscopic reversibility, that is, a collision which changes the velocity from v to v' if run backwards in time would change the velocity from v' back to v. This is true, of course, for real systems obeying Newton's laws, but due to the probabilistic nature of the present model can only be true in an average sense. However, this requires that if $v' = f(v)$, in the reverse collision $v = f(v')$ and hence $f = f^{-1}$. This condition, along with Eq. (2), can be substituted into Eq. (1) to yield

$$vP(v)dv = \pm v'P(v')dv' \tag{3}$$

after carrying out the v' integration. We note at this point that the velocity distribution is factorable into independent terms corresponding to each coordinate and we can use the simple result for the relative velocity that $P(v) \propto \exp(-\beta\mu v^2/2)$ where μ is the reduced mass of the pair and $\beta = 1/k_B T$. We can substitute this into Eq. (3) and use the boundary condition that v and v' must always be positive real numbers to find two solutions. If the positive sign is chosen in Eq. (3), we obtain the trivial result $v = v'$. If the negative sign is chosen we obtain the solution

$$\exp\left[\frac{-\beta\mu v^2}{2}\right] = 1 - \exp\left[\frac{-\beta\mu v'^2}{2}\right] . \tag{4}$$

We thus propose to use Eq. (4) to define $v' = f(v)$ which selects the outcome of a trial exchange and modifies the particle velocities if the exchange is accepted. Since this equation uniquely determines the change in kinetic energy for the exchange of a pair of sites, it completes the definition of the algorithm as outlined earlier in this section.

Only pairs with an initial v that is positive (i.e., the particles are moving toward each other) are considered for exchange, since pairs with negative v will not be expected to interact in the time step under consideration. On physical grounds, however, we would expect particles which successfully exchange to continue moving apart after the exchange, and those for which the exchange is rejected to "bounce" apart in an elastic collision. In either case, the final relative velocity will have changed sign. It is therefore necessary in order to maintain detailed balance that pairs with initial negative v end up with positive v even though no collision occurred. This can be thought of as a reflection of the constraint that both particles remain on the same sites during the update (i.e., they have an average relative velocity of zero during the time step), or of elastic collisions with their surrounding neighbors with which they are unable to interact.

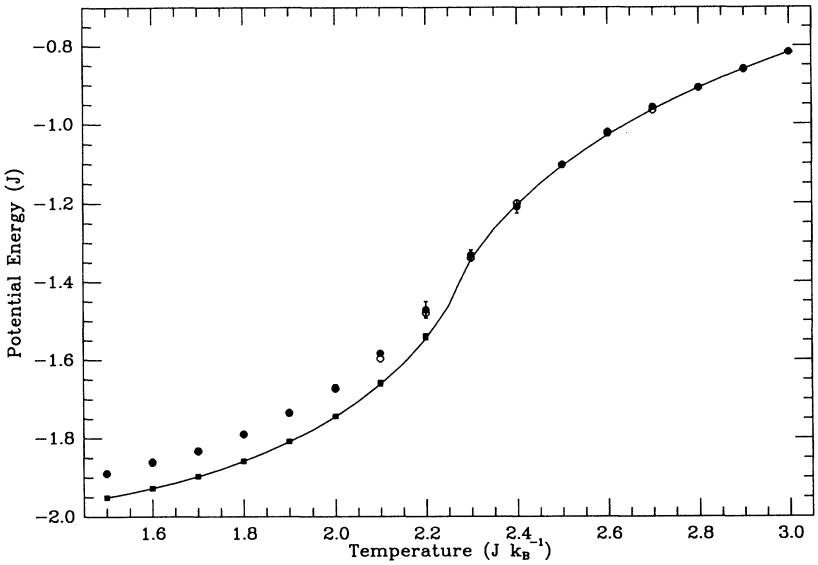

FIG. 1. Potential energy (in units of J) as a function of temperature (in units of Jk_B^{-1}). Solid symbols represent results from the dynamical MC algorithm and open symbols represent results of standard canonical MC simulations. Circles correspond to zero magnetization and squares correspond to exact single-phase magnetization below the critical point. The solid line is the exact value. Error bars for the dynamical MC results correspond to the standard deviation of three independent simulations. All simulations consist of 10^5 lattice passes with 100^2 sites. Open symbols and error bars where not visible are coincident with the solid symbols.

Note that on subsequent passes through the lattice the pairing of sites will be different and the particles will still on average be able to move in the direction of their velocities, as desired.

III. RESULTS FOR THE TWO-COMPONENT LATTICE GAS (ISING MODEL)

As a simple test of the dynamical MC algorithm, we performed a series of calculations on the two-dimensional Ising model, described by the Hamiltonian

$$H=-J\sum_{\langle n,n'\rangle}\sigma_n\sigma_{n'},\quad \{\sigma\}=\pm 1 \tag{5}$$

for which the exact partition function is known [13]. For simplicity, we assigned equal masses to the two components, and interpret the model as a binary fluid mixture. We also set the chemical potentials to be equal (zero magnetic field) and carry out simulations at fixed composition. Simulations were performed on a 100×100 square lattice with periodic boundary conditions. Each pass through the lattice consisted of one "collision" for every pair of neighboring sites. Results are presented in terms of the parameters which define the coupling strength J; site mass m; and lattice spacing l.

This distribution of site velocities was calculated and verified to be indistinguishable from the exact Maxwell-Boltzmann distribution over intervals an order of magnitude shorter than the equilibration time of the configuration. Calculated values of $(\beta/N)\langle E_k\rangle$ and $(\beta^2/N)(\langle E_k^2\rangle-\langle E_k\rangle^2)$ typically deviated from unity by less than 0.001 and 0.01, respectively, over most runs during which statistics were collected. The potential energy was found to equilibrate more slowly than in conventional canonical or grand-canonical simulations, however, reasonable results were obtained for runs consisting of 100 000 lattice passes taking ~ 7 h on an IBM RS6000 computer workstation. Calculated energies and heat capacities are plotted in Figs. 1 and 2, along with results

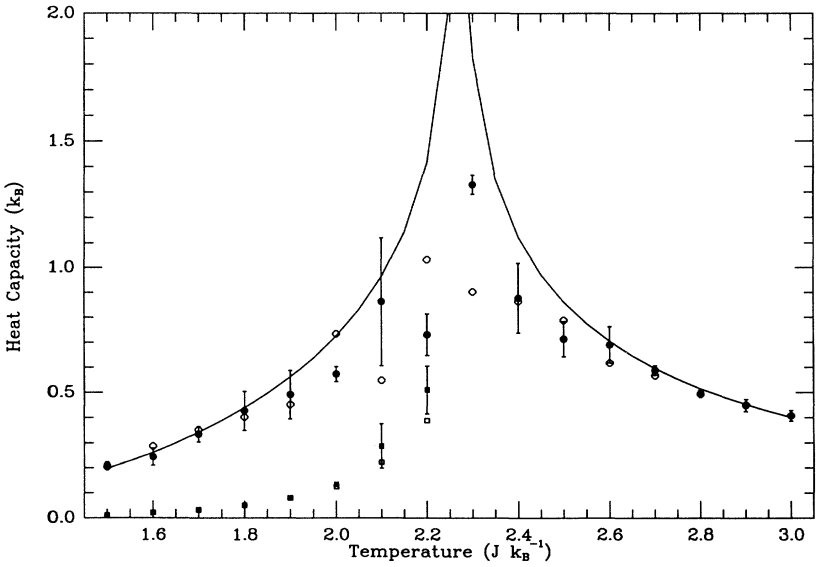

FIG. 2. Heat capacity as a function of temperature. Symbols are defined as in Fig. 1.

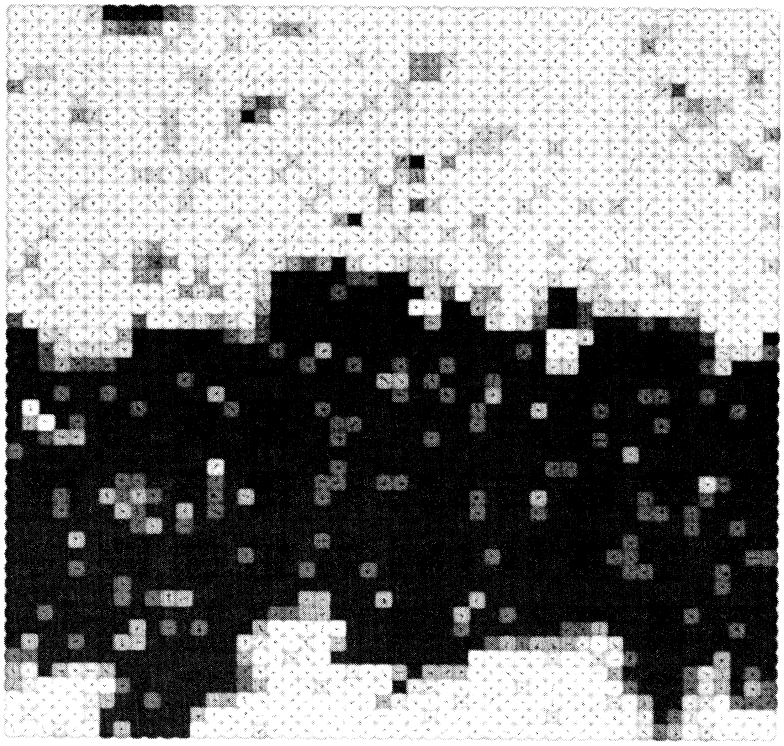

FIG. 3. Instantaneous configurations of the lattice from simulation. Each plotted square represents a 2×2 block of sites on the lattice. Squares are shaded from light to dark according to the number of light sites in the block from 0 to 4. Arrows represent the direction and magnitude of the average velocity of the sites in the block. (a) $T=2.0$, (b) $T=2.5$.

of conventional canonical MC calculations and the exact values. Results below T_c are shown for equal concentrations with phase separation, and with the exact single-phase mole fraction as input. Although this is known analytically in this case, it could in general be determined from grand-canonical simulations. These results indicate that the potential and kinetic energy distributions are equilibrated independently and that the separation of the two in deriving the algorithm is valid. It is important to note that below T_c the one-phase calculations significantly underestimate the heat capacity, although the energy is correct. This is due to the fact that with fixed concentration there are very few sites of the scarce component and this limits the scale of the fluctuations which occur. With phase separation, there is an interfacial contribution to the energy but the heat capacity is much closer to the correct value. This is because the two-phase coexistence allows for an essentially grand-canonical simulation of each phase. The heat capacity near T_c is underestimated by all methods, but this is due to the nature of critical fluctuations and it has been shown for standard MC simulations that longer runs and the use of finite-size scaling can provide much better estimates. The pair-correlation function $g(n)=\langle \sigma(0)\sigma(n)\rangle$ was also calculated and matches that obtained by conventional methods, confirming that the equilibrium structure has been correctly simulated. Typical configurations of the lattice are shown in Fig. 3 for temperatures above and below the critical point.

IV. VELOCITY AUTOCORRELATION FUNCTIONS AND SELF-DIFFUSION

The velocity autocorrelation function (ACF) can be calculated in two ways: directly from the velocities as $\langle \mathbf{v}(0)\cdot\mathbf{v}(t)\rangle$, and indirectly from the particle displacements as $\partial^2\langle[\mathbf{r}(t)-\mathbf{r}(0)]^2\rangle/\partial t^2$. In a Newtonian system where $v=dr/dt$ these definitions are identical. In the present model, however, it is important to note that $\langle \Delta\mathbf{r}\rangle$ for a particular exchange is determined by the relative velocity and not by the individual site velocities. Because of this, $\langle \mathbf{v}(0)\cdot\mathbf{v}(t)\rangle$ has a component due to the pair center-of-mass velocities which is not reflected in the resulting motion. For the remainder of this discussion, the velocity ACF will be defined as $\partial^2\langle[\mathbf{r}(t)-\mathbf{r}(0)]^2\rangle/\partial t^2$ so as to accurately describe the diffusion of the sites. Representative velocity ACF's are shown in Fig. 4. These functions show a deep minimum at short times on the order of a few time steps with a tail extending to longer times. This backscattering effect is a common characteristic of dense fluids, but it is expected that the long-time tail should ultimately be positive and proportional to t^{-1} for a two-dimensional fluid [14]. The presence of a negative velocity ACF extending to times much longer than typical collision times has been observed in MD simulation, and found to be more pronounced at high density [15]. Since the present model is essentially close packed, the results are consistent with this observed intermediate time scale. More detailed theoretical studies of mode coupling have indicated that while the dominant contribution to the long-time tail must ultimately be positive, there are other long-range contributions which are opposite in sign [16]. In the present case, the crossover between these competing terms may occur at times where the values of the velocity ACF are too small to be reasonably measured.

The velocity ACF's can be fit to the asymptotic form

$$\frac{\partial^2\langle[\mathbf{r}(t)-\mathbf{r}(0)]^2\rangle}{\partial t^2}\approx -ct^{-\alpha} \tag{6}$$

over the observable time of the simulation. Some representative values of the parameters c and α are shown in Table I. The results are shown for simulations with $\langle\sigma\rangle=0$. For $\langle\sigma\rangle\sim\pm1$, the system is essentially noninteracting and the correlations decay too rapidly to be reasonably characterized.

In two dimensions, where the integral

$$D=\tfrac{1}{2}\int_0^\infty dt\,\langle \mathbf{v}(0)\cdot\mathbf{v}(t)\rangle \tag{7}$$

diverges, the diffusion constant D is not well defined. Self-consistent definitions derived from mode-coupling theory have been proposed [17]; however, in the present case we proceed more directly by using the definition of a time-dependent diffusion constant

$$D(t)=\frac{1}{4}\frac{\partial\langle[\mathbf{r}(t)-\mathbf{r}(0)]^2\rangle}{\partial t} \tag{8}$$

and calculating $D(t)$ for a fixed time that is long enough to be representative of the limiting transport behavior. In practice, we chose to define the diffusion constant as the average value of $D(t)$ in the interval $1000<t<1200$. The root-mean-square displacement of the particles in this time interval is typically ~ 30 lattice spacings in each coordinate direction from their positions at $t=0$. This is a distance which is large relative to typical correlation lengths, but small enough so that the periodic boundary conditions have negligible effect. Diffusion constants calculated in this manner are shown in Fig. 5. As a comparison, we also calculate the diffusion constants in the same way using a standard canonical MC algorithm with no site velocities, but with the same number of attempted exchanges per time step as in the dynamical algorithm. In this case, the effective velocity ACF's decay much more rapidly and the diffusion constants are much larger, as shown in Fig. 5. Both curves show a distinct minimum just above T_c, as a result of the enhanced structural fluctuations which serve to constrain the motions of the particles. The results from canonical MC are qualitatively similar, but show a greater increase with increasing temperature. The results presented in Fig. 5 are for the symmetric case where $\langle\sigma\rangle=0$. Single-phase simulations

TABLE I. Fit parameters for the long-time tails of the velocity ACF.

Temperature (units of J/k_B)	$\ln[c/(\text{site/step})^2]$	α
1.5	4.3	0.52
1.8	4.2	0.56
2.1	3.7	0.70
2.4	2.0	1.15
2.7	1.2	1.50
3.0	1.3	1.60

below T_c have significantly higher diffusion constants for the rich component. The diffusion of the scarce component was not studied due to the much poorer statistical accuracy, but it would be expected to be small, and increase sharply through the critical point. Dynamical studies of this and related percolation phenomena will be reported in the future.

V. CALCULATION OF PRESSURE AND INTERFACIAL TENSION

We define the pressure in the model using the viral equation

$$p=\frac{1}{\beta}+\frac{1}{2L^2}\sum_{\substack{i,j\\(i\neq j)}}\mathbf{r}_{ij}\cdot\mathbf{F}_{ij}\ , \tag{9}$$

where L is the length of the simulation square and we define forces to exist only between colliding pairs of sites. For accepted moves, if the force is assumed to be a function of $|\mathbf{r}_{ij}|$, the virial term in Eq. (9) will vanish due to the fact that $\mathbf{r}_{ij}$ changes sign during the exchange. For collisions that do not result in exchange, $\mathbf{r}_{ij}$ is constant, and we define

$$\mathbf{F}_{ij}=\frac{2m\mathbf{v}_{ij}}{\tau} \tag{10}$$

as there is no change in potential energy and the collision is elastic. Here we introduce the reduced time step τ, such that $\langle|v|\rangle\tau=\langle P(v)\rangle$, that is, the average velocity is equal to the average rate of exchange of the sites. This is a constant determined by the algorithm and is equal to $0.5222\beta^{1/2}$. For all cases in which $\mathbf{v}_{ij}$ is negative, no exchange takes place and $\mathbf{v}_{ij}$ is made positive. Therefore $\langle\mathbf{v}_{ij}\rangle$ for collisions of this type is a constant determined by the distribution. Note that this is an attractive in-

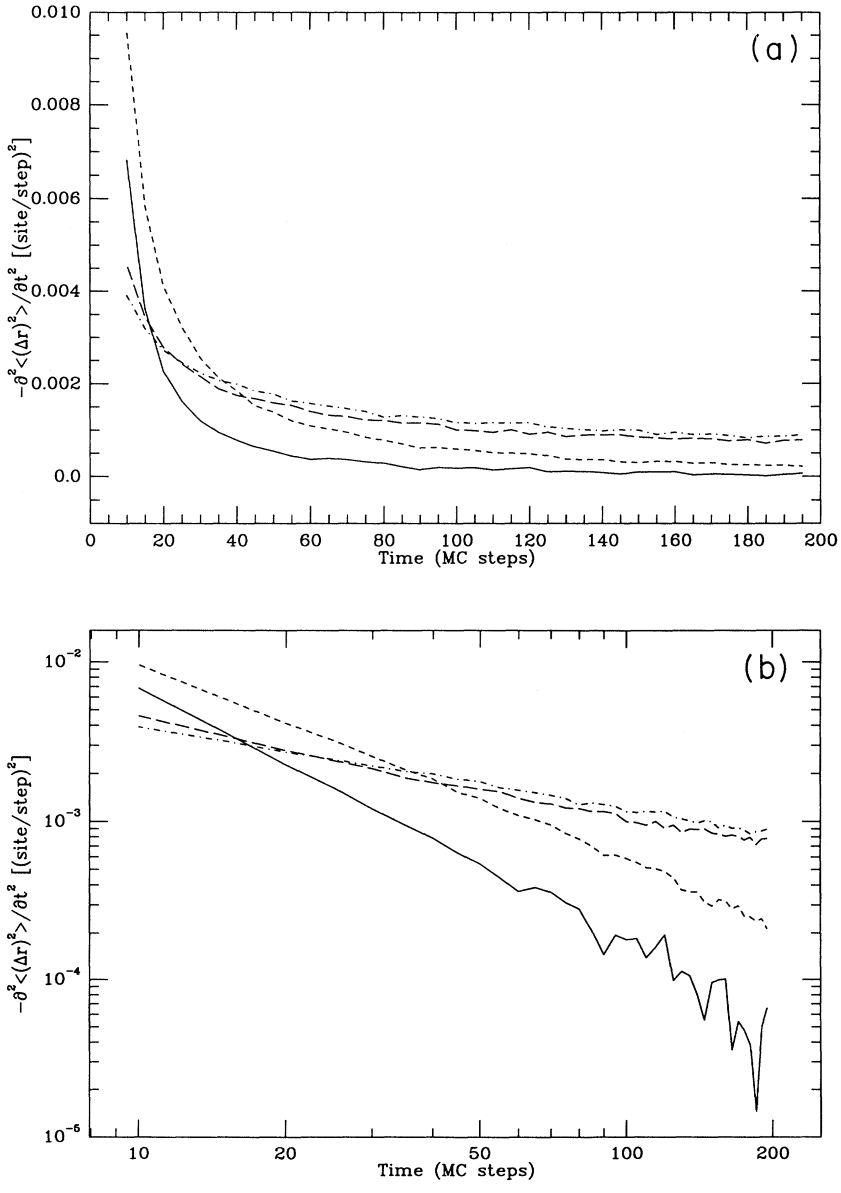

FIG. 4. Long-time tails of the velocity autocorrelation function. Lines correspond to the following temperatures: solid, $T=3.0$; short dash, $T=2.5$; long dash, $T=2.0$; dot dash, $T=1.5$. (a) Linear-linear scale, (b) log-log scale.

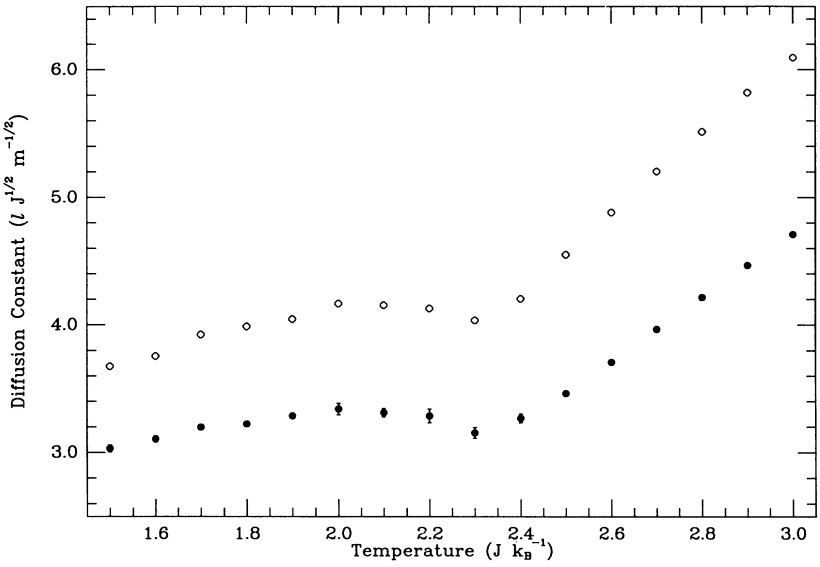

FIG. 5. Diffusion constant (in units of $lJ^{1/2}m^{-1/2}$) as a function of temperature. All points are with zero magnetization. Closed circles are from the dynamical MC algorithm and open circles are from standard canonical MC. Error bars are as in Fig. 1.

teraction and thus a negative contribution to the pressure. The remaining case corresponding to positive $\mathbf{v}_{ij}$ is that of an attempted move which is rejected, for which $\langle \mathbf{v}_{ij} \rangle$ is sensitive to the configuration. The pressure calculated in this manner is shown in Fig. 6. The pressure is a smoothly increasing function of temperature with a maximum slope at T_c. The pressure is also shown for phase-separated simulations where the effect of the interface can be seen to increase the overall pressure of the system.

The interfacial tension is defined by the relation

$$\gamma = \int_{-\infty}^{\infty} dy [p_y - p_x(y)] \tag{11}$$

for an interface parallel to the x axis [14]. In general, the orientation of the interface could be found by diagonalizing the pressure tensor, however, in the present simulation the interface is pinned to either the x or y axis by the periodic boundary conditions and thus we can use the simple formula $2\gamma = L|p_x - p_y|$, where there are two interfaces in the periodic cell. The interfacial tension is plotted as a function of temperature in Fig. 7, along with the exact result which is known analytically [13]. The agreement is reasonable, except at lower temperatures ($T < 1.5$) where the present calculation predicts $\gamma \propto T$ as $T \to 0$, because the calculated forces depend only on the velocities and are proportional to the temperature in real units. This is due to the fact that potential and kinetic energy are only exchanged in accepted moves and there is no provision for particles to be accelerated by arbitrarily large repulsive forces. In other words, the calculation of interfacial tension measures the relative acceptance rate of exchanges across the interface. If no such moves are accepted, then this method fails to determine the height

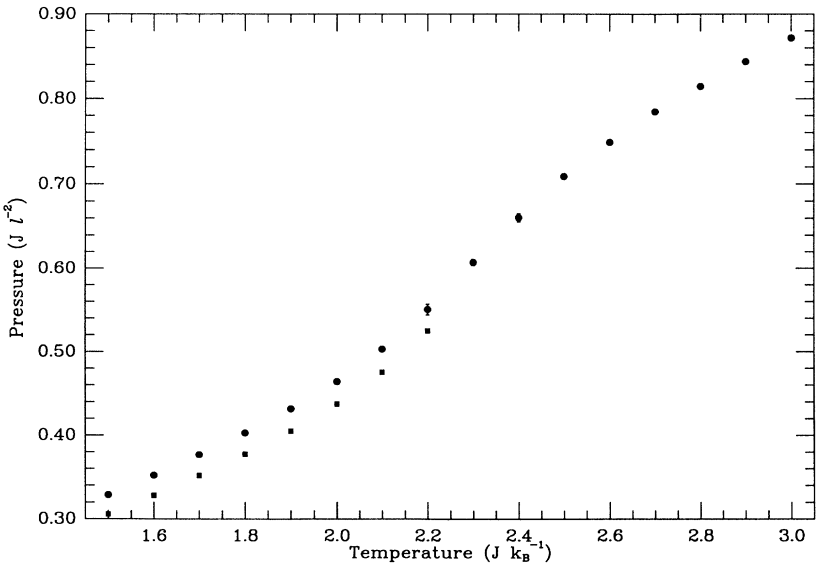

FIG. 6. Pressure as a function of temperature from dynamical MC simulation. Circles are with zero magnetization and squares are with exact single-phase magnetization. Error bars are as in Fig. 1.

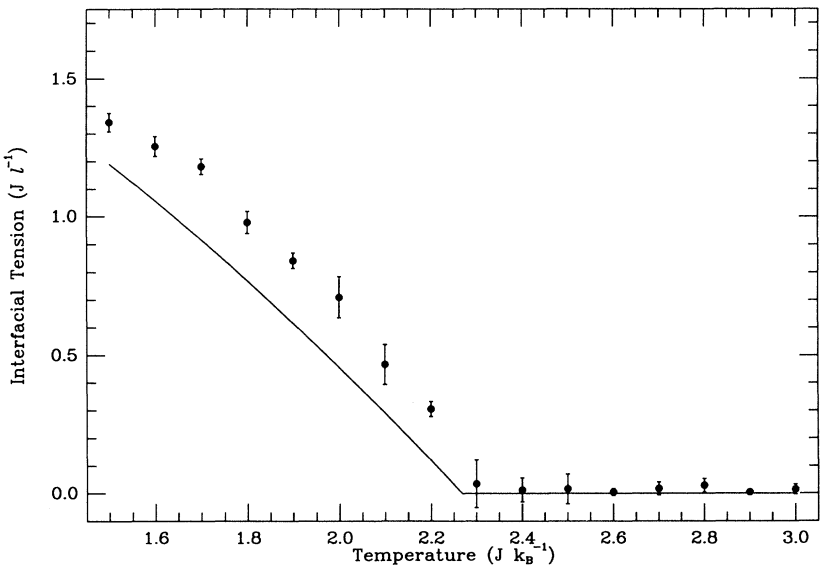

FIG. 7. Interfacial tension as a function of temperature from dynamical MC simulation. All points are with zero magnetization and error bars are as in Fig. 1. The solid line is the exact value.

of the barrier. Thus the method is only a reasonable estimate for systems in which the kinetic and potential energies are of comparable magnitude and the velocity distribution is perturbed to an extent that reasonably reflects the potential interactions.

The pressure in statistical mechanics is normally defined in terms of the derivative of the free energy with respect to density at constant β and N. In the case of the static Ising model this is of little use since the density does not enter into the problem in any meaningful way. There is therefore no exact function to which the results in Fig. 6 can be compared. The exact interfacial tension is not derived from Eq. (11) but instead arises from the calculation of the free energy of an antiferromagnetic lattice with an odd number of rows. The extent to which these different calculations of the interfacial tension agree indicates that both describe the same macroscopic property of the system.

Near the critical point, the fluctuations of the interface are comparable to the size of the periodic simulation square. It is thus possible for the interface, since it is free to move within the simulation, to change orientation on the time scale over which statistics are collected. It is thus important to calculate the interfacial tension over an appropriate interval so that reasonable averages can be obtained for the pressures, and yet the orientation of the interface remains fixed. As a consequence, however, large fluctuations slightly above T_c will produce nonzero values for the interfacial tension over the same interval, and the values below T_c are systematically high. The fluctuations are also restricted by the finite size of the system, and the calculated values of the surface tension can be improved by using a series of lattice sizes and extrapolating to $L=\infty$. The slope of the curve appears to be reasonably well represented, however.

The interfacial tension of the two-dimensional Ising model has also been calculated in MC simulation by Binder [18], using finite-size scaling arguments to determine the free energy of the interface. The results there are also systematically high, but more sophisticated analysis gives somewhat better results. The methods used in the traditional MC calculation, however, make use of the symmetry of the two phases and could not be easily applied to a system such as the model of microemulsion where the fluctuations in the order parameter are much different in the two coexisting phases and the chemical potential of the two-phase equilibrium may not be known exactly. Also, in such complex systems it may not be possible to obtain phase separation in smaller simulations, even with zero-order parameter. Finally, since the scaling method relies on spontaneous fluctuations, it is difficult to obtain good statistics at temperatures below about 1.8, and in three dimensions it is limited to a range of less than 10% of T_c. Thus the present algorithm, although somewhat crude, has the advantage of being much simpler to implement and would be expected to be applicable to a wider range of models over a wider range in temperature.

VI. SIMULATION OF A VELOCITY GRADIENT AND CALCULATION OF SHEAR VISCOSITY

The simulation of a constant velocity gradient was implemented by defining the velocities as being relative to an externally imposed flow in one of the coordinate directions. In the direction perpendicular to the flow, the magnitude of the flow is incremented by a fixed amount each lattice spacing. Since the lattice itself is not being sheared, this allows for an arbitrary shear to be applied uniformly at each time step. In addition, this method can be used across the periodic boundaries, since the flow at a site is only defined relative to its neighbors. Site exchanges parallel to the flow are unaffected since the velocity field is the same for both sites. For exchanges perpendicular to the flow, the velocity components in the flow direction are unchanged in absolute terms but their local values must be modified to take into account the difference in flow at the two sites. The relative velocity is treated the same as before, but there is now a transfer of

TABLE II. Results of simulations at a series of low shear rates at $T=2.5$.

Shear rate (relative units)	Shear viscosity (units of $\sqrt{mJ}/l$)	Internal energy (units of J)	Calculated temperature (units of J/k_B)
0.01	1.053	−1.11	2.505
0.02	1.066	−1.11	2.511
0.03	1.070	−1.12	2.518
0.04	1.068	−1.11	2.527
0.05	1.071	−1.11	2.536
0.10	1.105	−1.15	2.605

transverse momentum between the particles. Momentum is conserved, but since the kinetic energy is defined in terms of the local velocities, there is a change in kinetic energy resulting from this change in reference that is not a part of the Boltzmann factor which determines the acceptance or rejection of the move. There is therefore an increase in the calculated temperature due to the shear. Other methods of simulating shear use discrete displacements of the lattice sites at periodic intervals with an otherwise standard MC algorithm [19]. In this case it is necessary to estimate the heating effect and the effects of the discrete nature of the shear.

Using the conventional mechanical description of the shear, the applied force necessary to maintain the velocity gradient is proportional to the net transfer along the gradient of momentum in the flow direction. The shear viscosity is thus defined as

$$\eta = -\sum_{\mathbf{r}_{ij}=\hat{\mathbf{y}}}^{\text{acc}} \frac{m(v_{ij,x}-u)}{uL^2\tau} \tag{12}$$

for flow in the x direction with a gradient in the y direction, where the sum is over accepted exchanges in the y direction and u is the difference in flow between adjacent rows of the lattice. The shear viscosity was calculated at $T=2.5$ as a function of shear rate, and the results are shown in Table II, along with the calculated temperature and internal energy. The shear rate is expressed in relative units in which $\langle v^2\rangle=1$. At very low shear rates there is larger statistical error, and at high shear rates there is evidence of shear-induced structural changes in the configuration. In the intermediate range, though, the result is essentially constant. An instantaneous configuration corresponding to a shear rate of 0.10 in Table II is shown in Fig. 8. The configuration shows distinct parallel domains, which also suggests the onset of a shear-induced phase transition. However, in the present work we did not investigate high shear rates and the shear-induced shift in T_c. This would require maintaining a consistent temperature by rescaling the velocities. Instead, we chose to calculate shear viscosity as a function of temperature at a constant shear rate low enough so that the perturbation to the system is minimal and we are effectively in the limiting regime of $u\to 0$. The shear

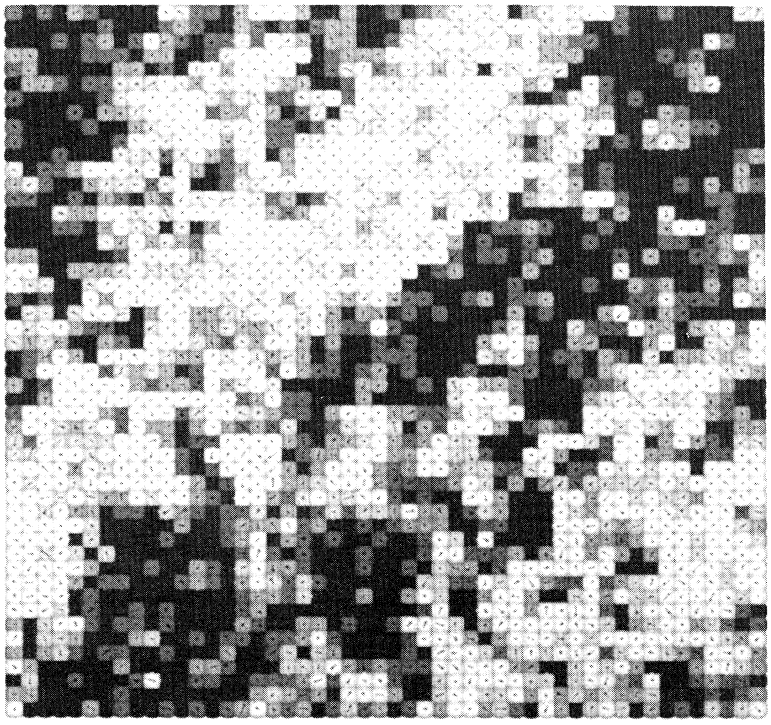

FIG. 8. Instantaneous configuration as in Fig. 3. The reduced shear rate is 0.10. Velocities shown are with respect to the flow velocity.

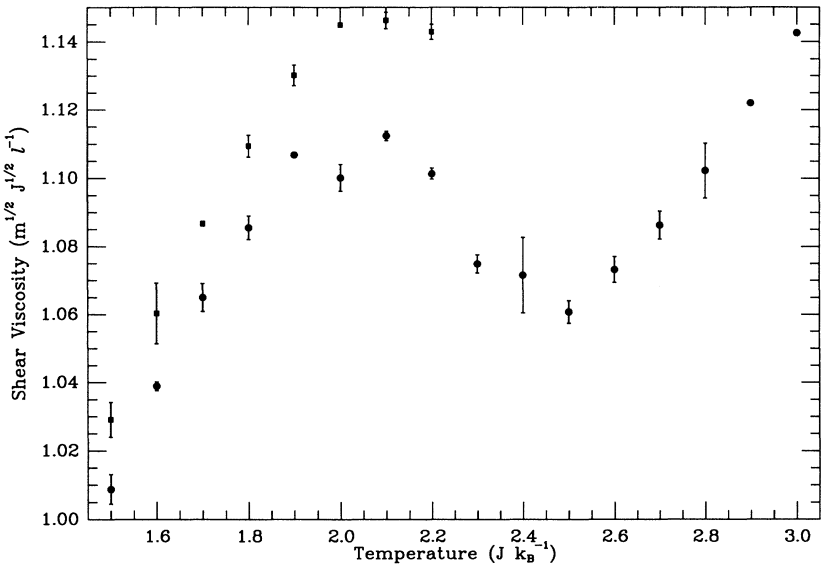

FIG. 9. Shear viscosity as a function of temperature from dynamical MC simulation. Symbols are as in Fig. 6.

viscosity calculated at a shear rate of $u = 0.03$ is plotted in Fig. 9. The increase in temperature in all cases was less than 1%. The calculated shear has a pronounced minimum near T_c that is similar in nature to the same feature in the diffusion constant plot. This is a reasonable result as the transverse momentum flow is expected to be determined by the diffusion of sites across the flow direction. Results are also shown for phase-separated simulations where the phase boundary is perpendicular to the flow direction. In this case the shear viscosity is somewhat higher as would be expected since the interface will resist the shear.

This algorithm can also be used to study forced flow without periodic boundary conditions (that is, with fixed walls) and around fixed barriers. Sites are introduced into the lattice which cannot exchange and which reverse the relative velocity of sties which collide with them. In this case, momentum is no longer conserved and must be periodically corrected along with the temperature. A typical snapshot is shown in Fig. 10, in which it can be seen that the barrier appears to wet the interface. This type of simulation will be investigated more thoroughly in the future. The algorithm could also be adapted to include vacancies which can be made to exchange with any

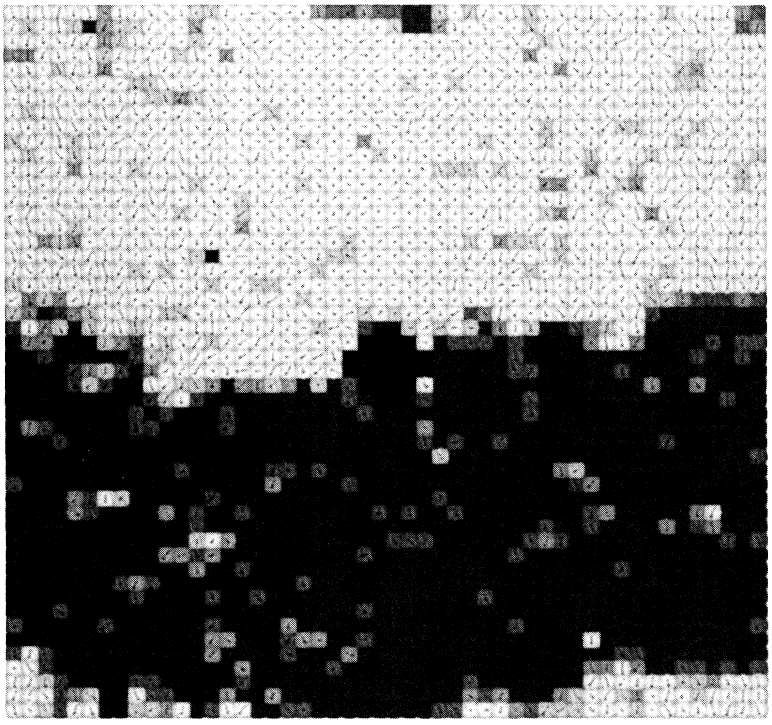

FIG. 10. Instantaneous configuration as in Fig. 3. The center black squares are noninteracting fixed sites. Velocities are shown with the net flow past the barrier included.

other sites moving towards them. Such a move would conserve momentum but perturb the potential energy and velocity distributions.

VII. CONCLUSIONS

We have introduced an algorithm for carrying out time-dependent Monte Carlo calculations for a lattice of interacting sites. We have performed a series of test calculations using this method to study the two-dimensional Ising model which reproduce the results of standard MC simulations. In addition, we have used this test case to demonstrate the calculation of dynamical quantities that are unavailable with standard methods. In particular, encouraging results are presented for the calculation of diffusion constants, interfacial tension, and shear viscosity using this algorithm.

The calculation of the diffusion constant is complicated, as expected, by the presence of long-time tails in the velocity autocorrelation function, however, preliminary calculations indicate that the problem is greatly reduced in the three-dimensional case. The calculated interfacial tension is compared to the exact results and although discrepancies exist due to finite-size effects and limitations of the algorithm, the agreement is generally quite good over a reasonable temperature range. The calculated restoring force in a simulated Couette flow is found to be proportional to the shear rate in the regime where the structure remains intact, leading to a simple calculation of the shear viscosity.

Further applications of the method are suggested, including the simulation of high shear rates, investigation of shear-induced phase transitions, and exploration of the phase diagram as a function of shear rate. Also possible is the calculation of driven flow around fixed barriers and in restricted geometries. The method can also be simply extended to consider components of different masses, including the possibility of massless vacancies such as those found in conventional lattice gases.

There are some issues remaining to be resolved, including the inclusion of collective motions and a more complete understanding of the hydrodynamic behavior of the system. However, the present work represents a promising beginning, and we feel that the algorithm presented here will lead to significant gains in the understanding and modeling of complex fluids.

ACKNOWLEDGMENT

The authors gratefully acknowledge financial support from the Packard Foundation.

---

*Present address: Box 6 Havemeyer, Columbia University, New York, NY 10027.

†Present address: Dept. of Chemistry, University College Dublin, Belfield, Dublin 4, Ireland.

[1] It is beyond the scope of this paper to present a complete review of these methods. An excellent introduction and bibliography can be found in M. P. Allen and D. J. Tildesley, *Computer Simulation of Liquids* (Oxford University Press, Oxford, 1987).

[2] J. R. Gunn and K. A. Dawson, J. Chem. Phys. **96**, 3152 (1992).

[3] J. R. Gunn and K. A. Dawson, J. Chem. Phys. **91**, 6393 (1989).

[4] B. Smit, A. G. Schlijper, L. A. M. Rupert, and N. M. van Os, J. Phys. Chem. **94**, 6933 (1990).

[5] Representative reviews can be found in Complex Syst. **1**, No. 4 (1987); and *Discrete Kinetic Theory, Lattice Gas Dynamics, and Foundations of Hydrodynamics,* edited by R. Monaco (World Scientific, Singapore, 1989).

[6] U. Frisch, B. Hasslacher, and Y. Pomeau, Phys. Rev. Lett. **56**, 1505 (1986).

[7] M. E. Colvin, A. J. C. Ladd, and B. J. Alder, Phys. Rev. Lett. **61**, 381 (1988).

[8] H. Chen, S. Chen, G. D. Doolen, Y. C. Lee, and H.C. Rose, Phys. Rev. A **40**, 2850 (1989).

[9] D. H. Rothman and J. M. Keller, J. Stat. Phys. **5**, 1119 (1988); G. W. Baxter and R. P. Behringer, Phys. Rev. A **42**, 1017 (1990); J. M. Vianney and A. Koelman, Phys. Rev. Lett. **64**, 1915 (1990).

[10] A. B. MacIsaac, D. L. Hunter, M. J. Corsten, and N. Jan, Phys. Rev. A **43**, 3190 (1991).

[11] See, for example, *Computer Simulation Studies in Condensed Matter Physics,* edited by D. P. Landau, K. K. Mon, and H.-B. Schüttler (Springer-Verlag, Berlin, 1990).

[12] M. Creutz, Phys. Rev. Lett. **50**, 1411 (1983); M. Creutz, Ann. Phys. (N.Y.) **167**, 62 (1986).

[13] L. Onsager, Phys. Rev. **65**, 117 (1944); B. M. McCoy and T. T. Wu, *The Two-Dimensional Ising Model* (Harvard University Press, Cambridge, MA, 1973).

[14] See, for example, J.-P. Hansen and I. R. McDonald, *Theory of Simple Liquids* (Academic, London, 1986).

[15] J. Talbot, D. Kivelson, G. Tarjus, M. P. Allen, G. T. Evans, and D. Frenkel, Phys. Rev. A **65**, 2828 (1990).

[16] T. R. Kirkpatrick and J. C. Nieuwoudt, Phys. Rev. A **33**, 2658 (1986); B. Kumar and G. T. Evans, J. Chem. Phys. **90**, 1812 (1989).

[17] D. Frenkel and M. H. Ernst, Phys. Rev. Lett. **63**, 2165 (1989).

[18] K. Binder, Phys. Rev. A **25**, 1699 (1982).

[19] C. K. Chan and L. Lin, Europhys. Lett. **11**, 13 (1990).

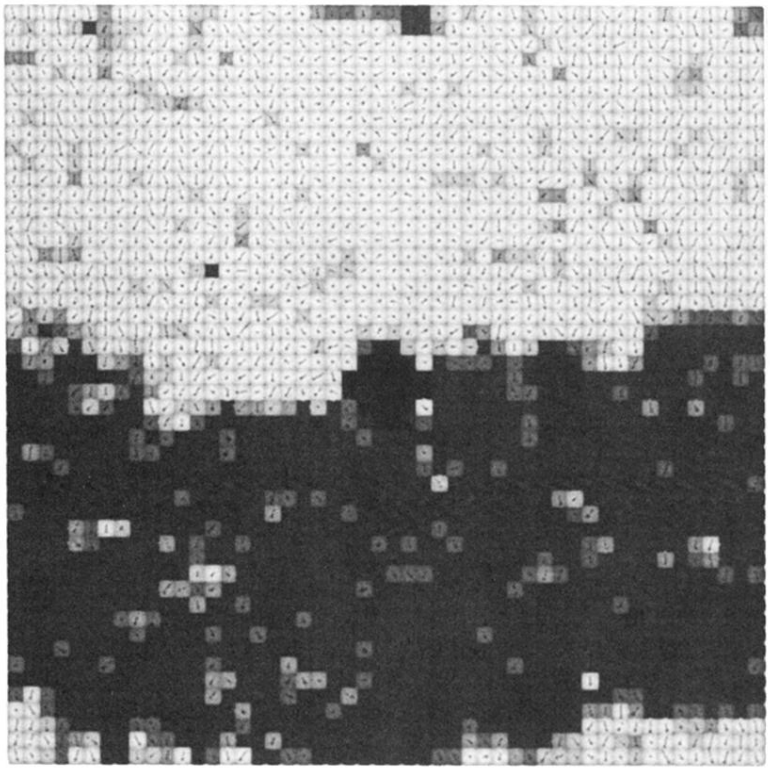

FIG. 10. Instantaneous configuration as in Fig. 3. The center black squares are noninteracting fixed sites. Velocities are shown with the net flow past the barrier included.

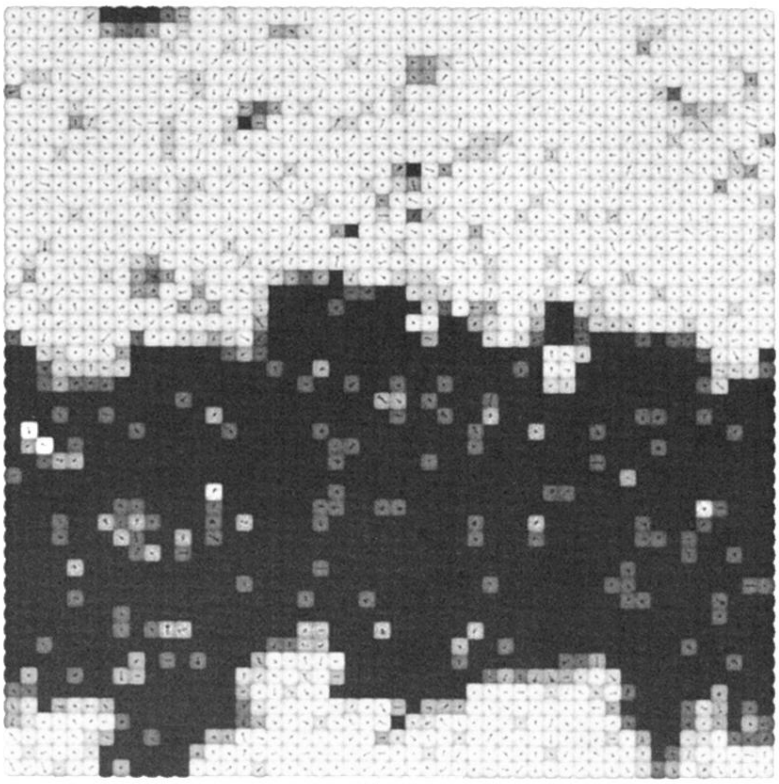

(a)

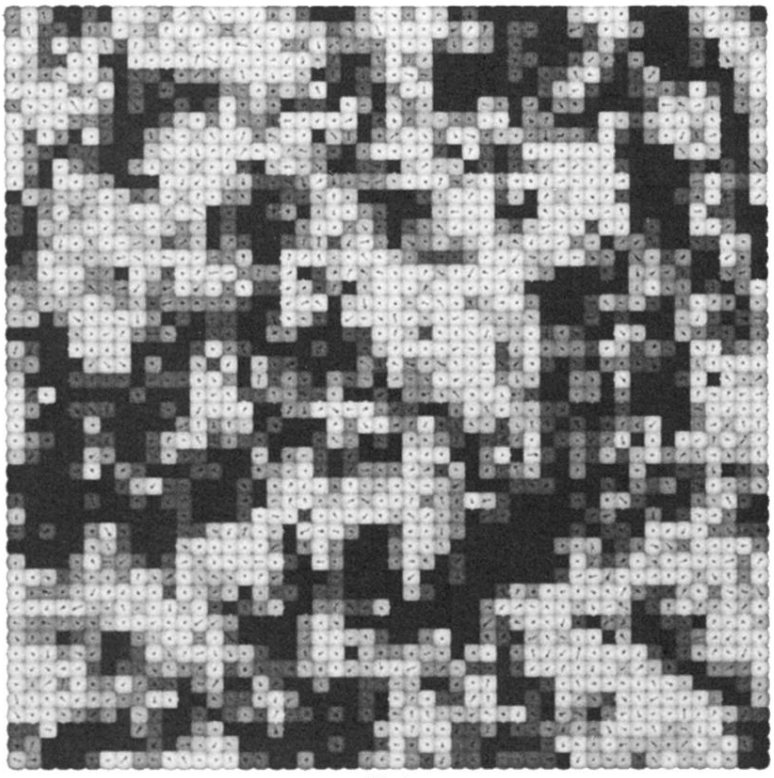

(b)

FIG. 3. Instantaneous configurations of the lattice from simulation. Each plotted square represents a 2×2 block of sites on the lattice. Squares are shaded from light to dark according to the number of light sites in the block from 0 to 4. Arrows represent the direction and magnitude of the average velocity of the sites in the block. (a) $T=2.0$, (b) $T=2.5$.

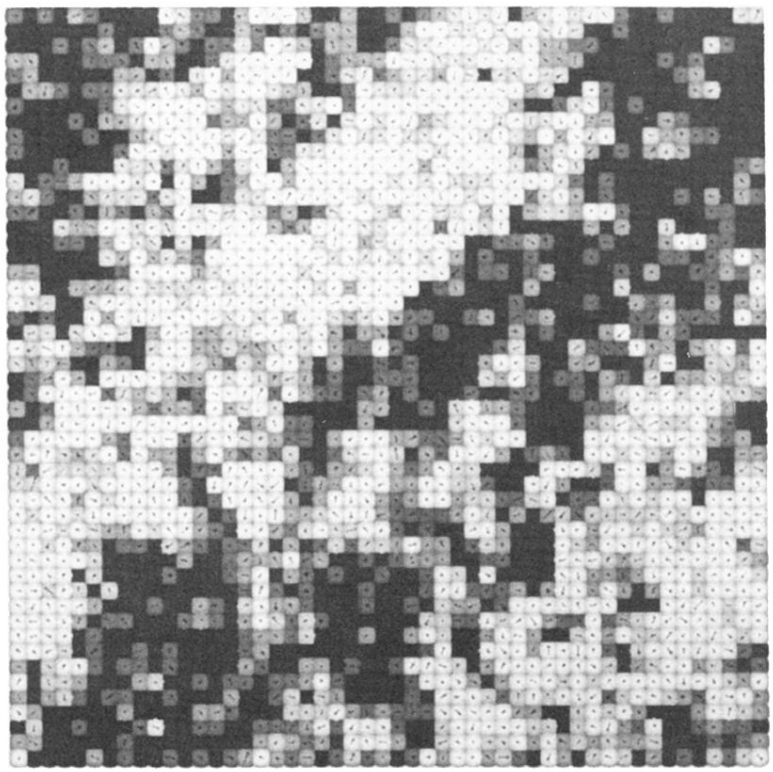

FIG. 8. Instantaneous configuration as in Fig. 3. The reduced shear rate is 0.10. Velocities shown are with respect to the flow velocity.